Journal of Himalayan Earth Sciences Volume 53, No. 1, 2020 pp. 95-117

Spatiotemporal change analysis of snow cover in response to climate (in-situ temperature) over the Upper Indus Basin, Pakistan

Garee Khan[1,2,3*], Chen Xi[1,2*], Babar Khan[4], Javed Akhter Qureshi[3], Hawas Khan[3] and Iram Bano[3]

[1]*State Key Laboratory of Desert and Oasis Ecology, Xinjiang Institute of Ecology and Geography, Chinese Academy of Sciences, Urumqi*

[2]*University of Chinese Academy of Sciences, Beijing*

[3]*Department of Earth Sciences, Karakoram International University, Gilgit-Baltistan*

[4]*World Wide Fund for Nature, Pakistan, GCIC Complex, NLI colony Jutial, Gilgit*

**Corresponding author's email: gareewwf@gmail.com*

Submitted date:18/12/2019 Accepted date:10/03/2020 Published online:30/03/2020

Abstract

The hydrologiest are debating on the rise in global glacier melting. However, the situation in Karakoram glaciers seems not the same. Therefore, it is essential to measure the status of snow in the Karakoram region of (GB; Gilgit-Baltistan) Pakistan. To this end, the current study examines the dynamics of snow cover using Moderate Resolution Imaging Spectroradiometer (MODIS) 8-days sow-cover in response to in-situ meteorological indicators from four high altitude automatic weather stations in Upper Indus Basin (UIB). The results conclude that the 8-days snow cover images not only show the qualities of MODIS (high resolution) images it's also characterized the high accuracies for snow-cover classification (~85 to 95 %). We analysed the snow-cover dynamics in the UIB and computed the maximum quantity of snow cover days (SCD) in a year that shadowed an increasing trend from 2000-2014, with an increase in snow-covered area (SCA) of 45.04% to 59.26% of the total land area of GB. Besides, there is a slightly decreasing trend observed in the SCA of Hindukush, and Himalayan mountains region in the last 15 years, due to increases in temperature and precipitation. Spearman's correlation analysis is also obtained between monthly and annually snow-cover changes (snow accumulation /depletion over six elevation zones above 2000 m elevation) and temperature. The month of January shows decreasing trends for five elevation zones out of six zones below 6000 m elevation. In spring, particularly in March shows a decreasing trend for two zones above 5000m elevations, while shows increasing trend in autumn for three zones above 4000 m elevation. A negative trend observed between monthly SCA and Khunjerab area (mean temperature and precipitation), and similar results are also noted for the remaining three regions such as Deosai, Naltar and Shandoor of UIB. The study suggests that, in the UIB region, climate change also employ a significant influence on regional SCA and days, as well as the distribution of snow-cover. These findings help for the forecasting of seasonal flow in the area and signifying snow-cover as a possible predictor of climate change.

Keywords: Climate change, Glacier, Karakoram, MODIS, Snow cover area.

1. Introduction

Snow is an essential component of the biosphere, and it significantly affects the hydrological regimes of the atmosphere, due to reflectance (high) values and little thermal conductivity. Snow plays a vital role for hydrological processes such as evaporation, condensation, precipitation, interception, infiltration, percolation, transpiration, runoff, and storage, a large portion of the water supplies originates from perennial and non-perennial snow-melting at high altitudes hilly watersheds (Barnett et al., 2005). This is mostly acceptable for the upper Indus basin (UIB), where seasonal snow and glacier-melts are the primary sources of freshwater supply to over 1.4 billion people in the Himalaya, Karakoram and Hindu Kush (HKH) (Immerzeel et al., 2010). Primarily available water uses for domestic, agriculture, power generation and industrial (Hasson et al., 2013). The contribution of snow and glacier-melt to the Indus river system has not yet been investigated accurately. About 40% of snow-melt water flow contributes to UIB based on Hydrological modelling by Immerzeel et al. (2009), and many uncertainties exist in the applied modelling techniques. In contrast, the importance of snow-melt for the Indus river system, Konz et al. (2010) concludes that it is vital to quantify precise snow-cover distribution patterns in the region. Since snow cover analysis is essential for the adjustment and justification of distributed hydrological models, as well as for forecasting of regular water flows.

Snow and glaciers cover a more substantial portion of Himalayan Mountains (Maske et al., 2011), have noticed significant temperature increased during recent periods (Diodato et al., 2012), while the region is more sensitive in terms of climate change and global warming (Maskey et al., 2011). About 16% of annual snow cover (average) was decreased over the Himalayan region in the period 1990-2001 (Menon et al., 2010), similar results also observed by Immerzeel et al. (2009), for HKH region. In the same way, most of the glaciers in the Himalayas have been fastly and losing their ice-mass since (Ad 1300- 1850) end of Little Ice Age. Instead of this, current studies show an account of average ice mass acceleration since the mid of the 1990s (Bolch et al., 2012). The UIB has (In contrast) different type of climatic conditions, presenting decreasing trend of minimum summer temperature and increasing precipitation (Fowler & Archer, 2006). Treydte et al. (2006) observed that the last century was the drizzliest era in this region. Glaciers of Karakoram have indicating stable or accumulation of ice-mass during the previous decade, as compared to the other areas of the world ice reserves (glaciers) (Bhambri et al., 2013), namely Karakorum Anomaly. Local people also confirmed this phenomenon (changes in climate) in the UIB area (Gioli et al., 2014). Under such diverse hydrological regimes, mainly snow-cover distribution is unknown, it is essential to study uncertainties in the context of present and future water resource management.

It is hard to evaluate the snow cover variation and distribution on sub-catchment level, and also on regional scales due recently (short-length) installed sparse high altitude hydro-meteorological stations within UIB region. Snow-cover surveys are also not easy or possible in the UIB region, due to massive area are remote, inaccessible and harsh weather, as well as complex terrain and its demographic settings (Maskey et al., 2011). Any effort to forecasting the chance of UIB snow and ice/glaciers will remain something other than undisputable. Moreover, as snow landscapes have a high degree of inconsistency, it necessary to mapped using high-resolution (temporal) satellite images, contrasting glaciers, which require moderate to high resolution. For that, the integrated technique of RS; Remote Sensing, and GIS; Geographical Information System (Data) play a vital role in snow-cover mapping, especially in remote and inaccessible areas (Tong et al., 2009).

Furthermore, acquired data offer an exclusive environmental data for snow area mapping, analysis, and provide results for effective management of snow-capped areas (Thirel et al., 2012). Few examples of satellite data usage are Moderate Resolution Imaging Spectroradiometer; MODIS (Aqua and Terra Data). The Advanced Very High-Resolution Radiometers (AVHRR) or the Interactive Multisensor Snow and Ice Mapping System (IMS) for snow-covered monitoring, which includes variability of spatial data products from AVHRR, GOES, and SSMI (Roy et al., 2010). However, available snow (satellite) data have many limitations, such as barrier of mixed (spectral reflectance values similar with ground objects) snow area with dense forest, vegetation, surface heterogeneity especially in mountainous region, as well as cloud covers hindering in way of surface view (Hüsler et al., 2014). From the study of the literature review of snow cover mapping methods, using remote sensing data have its limitations and advantages (Dietz et al., 2012). Unfortunately, the satellite sensor has limited ability to retrieve direct information from ground snow-cover, like SD; snow depth and SWE; snow water equivalent. Currently, available information about SD/SWE observations shows significant data inconsistencies Hasson et al. (2014) and their available resolution is too low (25km), is not suitable for representing snowy mountainous regions. It hindrance in the way of an accurate analysis of the SWE in the mountainous areas.

Recent studies about snow-cover change for Hunza, Astor, Shigar and UIB (Immerzeel et al., 2009; Samreen et al., 2014; Tahir et al., 2011) have used the MODIS (8-days) maximum snow data, which is partly correct Xie, Wang, and Liang (2009), missing of climatic parameters correlation and cloud data gaps. Hence, the primary constraint is clouded for accurately acquired satellite data, their existence in MODIS snow data restrict fair snow assessment and hosts data uncertainties in the investigation (Hasson et al., 2014). To highlights the need to improve satellite snow-products by filling/removing cloud data gaps before use for further data analysis. Many researchers have been shown that the MODIS snow product accuracy is very high under cloud-free data (Wang & Xie, 2009). However, any day (given), a large share of the Earth's may be covered by clouds, which reduce the fitness of snow monitoring by MODIS snow data (Hall et al., 2010). Recent years, many procedures have been established by the researchers for clouds removal from satellite imageries, such as for MODIS snow products (Xie et al., 2009). In which including snow-line (SNOWL) by Parajka et al. (2010), multi-sensor combinations by Foster et al. (2011) and temporal deduction methods by Hall et al. (2010). Such methods are beneficial for reducing the impact of high clouds obscuration from the MODIS data to monitoring SCA (snow cover area). In this study, Landsat TM (Thematic Mapper) data used for authentication of MODIS (8-days) snow product, and results of the data used for clouds removal by using the rigorous non-spectral technique. The enhanced and improve or cloud-free images were used for measurement of snow-cover dynamics at different elevations zones for future available water resource management and hydrological modelling in terms of Diamer-Basha Dam. In this paper first time, we present detailed picture of temperature and precipitation effect on snow-cover over the study area above 2000 m from four high altitude automatic weather stations data (AWS). Also, we investigate Spearman's correlation analysis between monthly snow-cover and in-situ weather datasets (mean precipitation and temperature) used for the better organization of water resources of the region for future prespectives. However, previous researchers have focused specifically on snow area monitering and mapping for short-time period and have little focus on the association between climate and the environmental snow area changes, particularly variation of temperature trends in the study area.

The study validates the correctness of the MODIS 8-day snow data, to analyse and inspect the snow-cover dynamics in terms of climate change in the UIB (Gilgit-Baltistan) from 2000 to 2014 with MODIS data.

2. Study area

The HKH region extent varies up to 2000 km (length) along East to West with different climatic conditions, including changing topographic terrain and precipitation (Bocchiola & Diolaiuti, 2013), manipulating the condition and development of cryosphere. This massive mountain and freshwater resource provide water for food security and power generation. About 50% of freshwater of Indus River comes from the snow and glacier melting in great Karakoram (Immerzeel et al., 2010). The present analysis of snow dynamics was carried out for Gilgit-Baltistan (Fig. 1).
Gilgit-Baltistan (GB) of Pakistan comprising of high peaks of Himalaya, Karakoram and the Hindu Kush, on the north. Western Himalayas exist on the south. GB is situated in extreme north of the Country (Pakistan) bordering with China, India and Afghanistan internationally, on north (35° 37' 00" N) and East (72° 75' 00" E) covers an expanse area of 72,496 Km2 (27,799 square miles) with elevation varying between 1000m and 8,611 m ASL. Major land uses glaciers (28.7%, n=72496 km2), agricultural land (1.36 %), forests (3.2 %), rangelands (32 %), barren lands i.e., rocks/clips and bare soils (34.4 %) and others including streams and rivers (0.43 %) of total area (Khan, 2013).

Geographically, climatically, and biologically the area represents a land of trans-Himalayan character, where monsoon rain and seasons of the plain are almost totally absent. Maximum precipitation occurs in the form of snow between 5000 and 6000 m ASL (Hewitt, 2007). Its significant parts lie within the watersheds of the Himalayas, Hindu Kush and Karakoram. The land lies among high mountains, snow-capped peaks and thin gorges opening their face to the valleys. The region is unique in its topography. Glaciers, ice and snow, are the only sources of freshwater for 160 million people living in the plains of Pakistan, as the nine tributary rivers originating from HKH mountains keep the Indus flowing for drinking, irrigation, fisheries and power generation downstream (Khan, 2013). According to SHIP-WAPDA; Snow and Ice Hydrology Project of the Water & Power Development Authority, the area has 80-90% of the total snow and ice cover (Ashraf et al., 2012). Non-perennial snow and glacier-melt contribute to more immense proportions during summer water discharge into the Indus River System.

2. Data

2.1. *Snow data*

The MODIS satellite is operating two sensors, Terra and Aqua. MODIS Terra satellite data acquired February 2000 onward was used for this study. The viewing swath width of the MODIS sensor had 2330 km with the capability to view the entire earth surface of the world within two days. It had about 36 spectral reflectance bands with a range from 0.405 to 14.385µm. Its spatial resolution is 500m x500m. The MODIS Terra L3 (MOD10A2) 8-day version 5 global snow products accessible from the National Snow and Ice Data Center (NSIDC) were used (http://nsidc.org/data/modis/data_summaries). MODIS snow data had high reflectance in visible bands 4 and 6 and also used these bands to calculate NDSI of the study area (Lopez et al., 2008). The data geodesic grid in sinusoidal map projection, and each tile divided by 10 degrees square approximately at the earth equator. The data period started from the first day of each year, and it covered up to the fifth day of the first month next year. The MODIS product showed maximum snow cover area in the specified eight days. The corresponding tile used for this study was 23hv5 & 24hv5, a series of 681 tiles from 1st March 2000 to 31 December 2014.

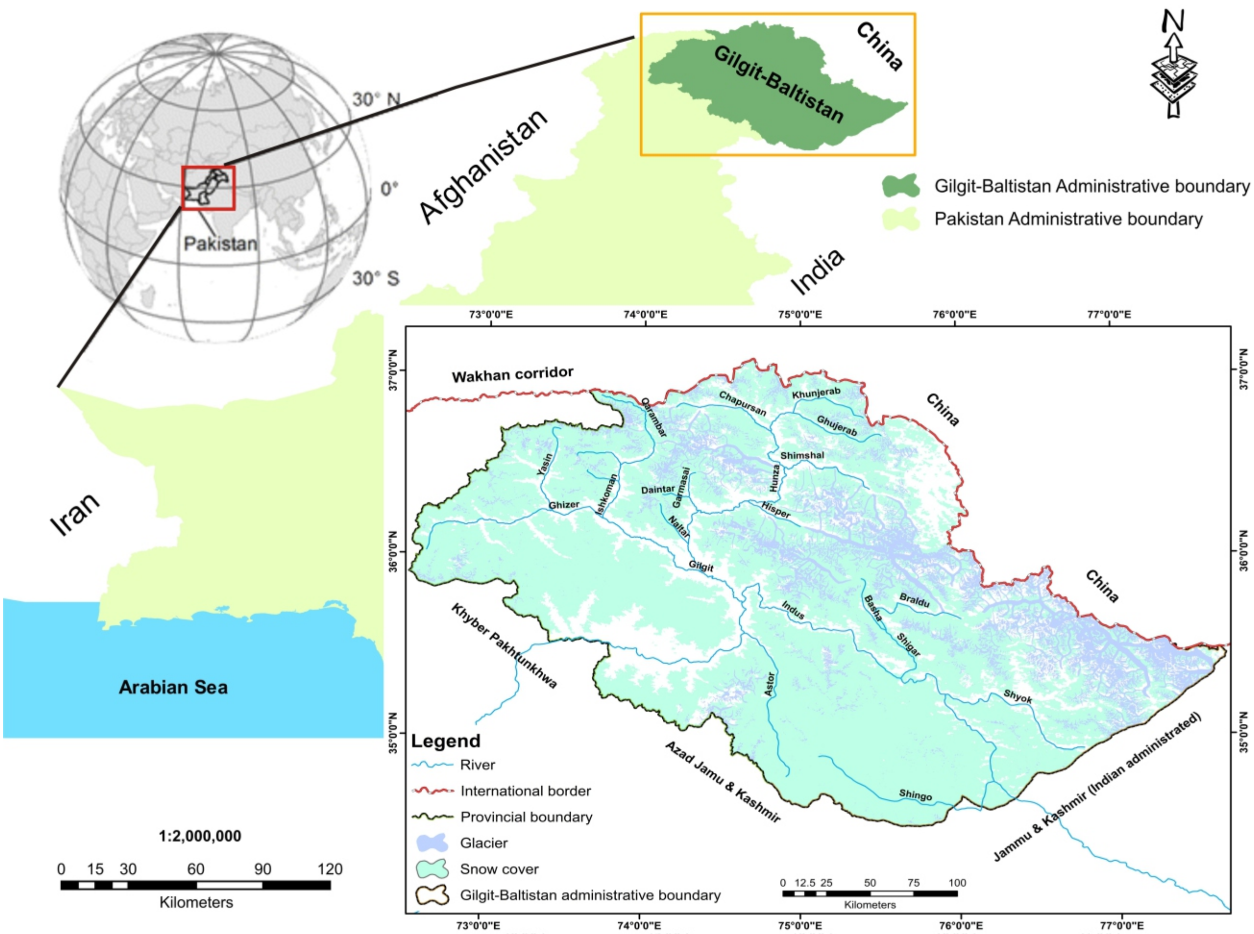

Fig. 1. Study area map with hydrological and weather stations (Source: MODIS Terra September 2010)

2.2. *Satellite images*

Previous studies used different type of proxy datasets for authentication of MODIS snow data. used ASTER; Advanced Spaceborne Thermal Emission and Reflection Radiometer images for validation of MODIS (8-days) terra images. used temperature data for constructed snow cover validation. Similarly, used Landsat TM and ETM+ images for 2001 to 2003 for daily Terra and Aqua snow product. In this study used Landsat TM images for 2000-2014 (downloaded from USGS geo-portal (Glovis online archive; http://www.glovis.usgs.gov) for MODIS (8-days) snow product. These images cover maximum snow-cover extent for both seasons (accumulation and ablation) of the study area (Fig. 2). Detail of Landsat TM images as given in Table 1.

Table 1. Landsat images used for validation

Scene no	Sensor	Day	Path	Row
Tile1	TM	11/15/2010	147	35
Tile2	TM	12/10/2011	148	35
Tile3	TM	3/28/2009	148	36
Tile4	TM	10/7/2010	149	34
Tile5	TM	8/27/2009	149	35
Tile6	TM	10/17/2010	149	36
Tile7	TM	8/27/2009	150	34
Tile8	TM	9/19/2009	150	35
Tile9	TM	9/19/2009	150	36
Tile10	TM	8/28/2010	151	35

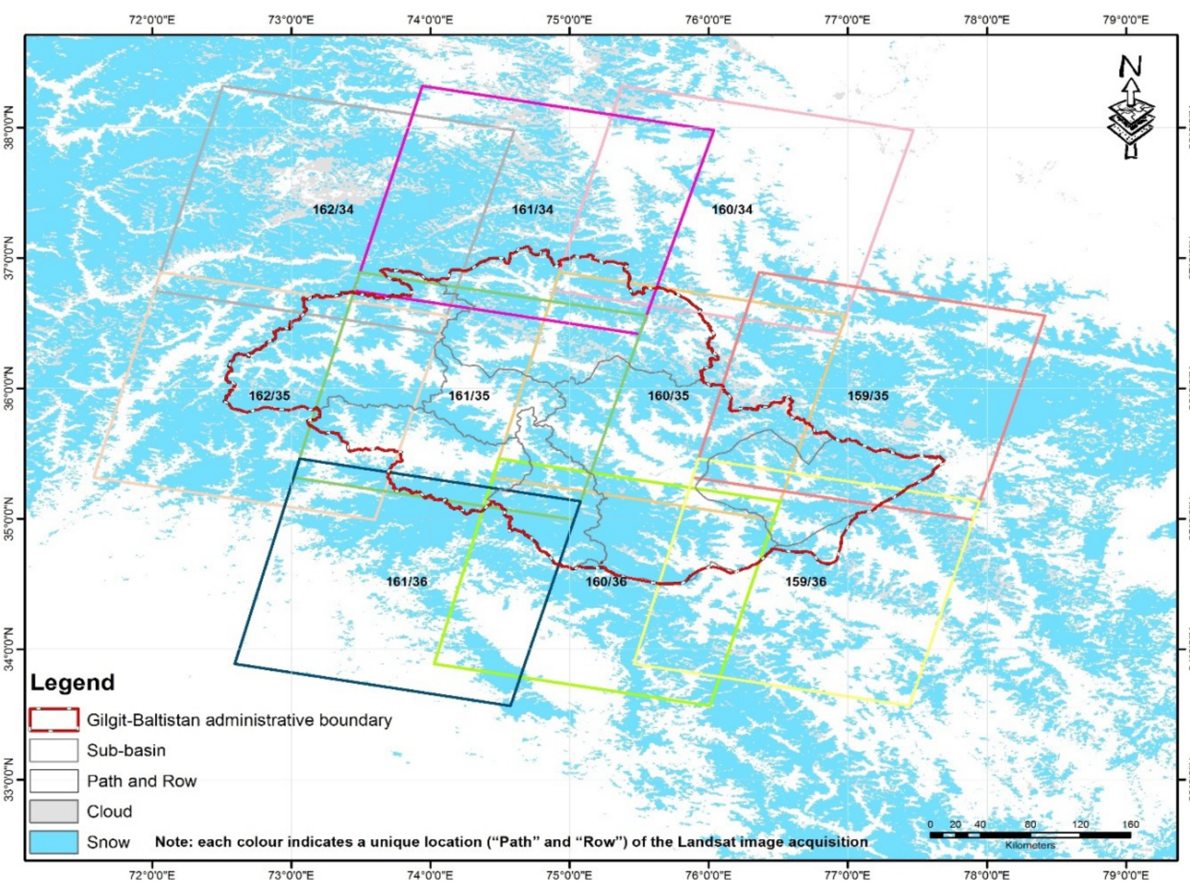

Fig. 2. Landsat data used for accuracy assessment of MODIS snow data, cover most of the study area with maximum snow extent.

2.3. Digital Elevation Model (DEM)

The gap-filled with ASTER 30m spatial resolution GDEM was acquired from the NASA reverb geo-portal http://reverb.echo.nasa.gov was used to extract the boundary, watershed and six different elevations zones, i.e., Zone I (<2000 m), Zone II (2000-3000m), Zone III (3000-4000m), Zone IV (4000-5000m), Zone V (5000-6000m), and Zone VI (>6000m) for the study area, derived from DEM with Spatial Analyst tool in ArcGIS (ESRI, 2011). DEM was also resampling to the resolution (500m) using the nearest-neighbour interpolation procedure for the extraction of required topographic features.

2.4. Climate data

The in-situ temperature data (mean monthly temperature and precipitation) available for four high altitudes Automatic Weather Stations (AWS) in UIB area of Pakistan, i.e. Deosai, Naltar, Khunjerab, Deosai and Shandoor, for the last 15 years (2000–2014) were acquired from the WAPDA; Water and Power Development Authority, GoP; Government of Pakistan (Table 2). Mean monthly temperature was used to compute the Spearman's rank correlation coefficient for the study period.

3. Method

3.1. Snow cover change analysis

MODIS 8-day snow data (.HDF) format with sinusoidal map projection data gridded provided by the MODIS satellite required further processing procedures to be used for better results. MODIS snow data also contained significant percent (>10%) of clouds specifically in monsoon season, if not processed, these clouds might directly effect on the snow cover area/extent. The pixel data (images) with higher (>10%) cloud cover were further processed to eliminated clouds by using the linear interpolating method in between previous and next cloud-free images (Tahir et al., 2011). All the cloud-free satellite images from the year 2000 to 2014 were processed with ArcGIS tools. Images were mosaicked and converted into Tiff format. Further, all mosaicked tiles were converting its (re-projected) into a projected coordinate system (UTM 43N) with WGS 1984 for further analysis. Calculate the NDSI values from satellite data, Visible band four values (0.545-0.565 m) and Shortwave infrared band 6 (1.628-1.652 m) were used (Bashir & Rasul, 2010) in this study.

Normalized difference snow index (NDSI): To identify snow and other topographic features from satellite imageries, snow-cover mapping algorithm NDSI was applied on visible bands 4 and band 6:

$$NDSI = \frac{band4(visible) - band6(SWIR)}{band4(visible) + band6(SWIR)} \quad \mathbf{1}$$

Generally, the index value of NDSI varies from -1 to +1. To separate the snow-cover area (SCA) from other land features, the set value of NDSI is ≥ 0.1, with the condition of values varying from 0.1 to 1.0. When NDSI values (≥ 0.1) were used, the classified imagery results showed some snow-free classes into the snow (dense coniferous forests patches and water bodies). To reduce the classification errors from the imagery with NDSI method, in this study we used threshold value ≥ 0.4 for NDSI calculation to remove or eliminated other features classes clearly from snow (Klein & Barnett, 2003; Tait et al., 2001).

MODIS dataset was classified into two classes, such as snow and no-snow. Based on available datasets, calculated the image area with the help of different spatial analysis (Fig. 3).

3.2. Validation and accuracy assessment

Global Positing System (GPS) based 90 ground random sampling points were gathered from the field during the winter period (high snow accumulation months; December-March) of 2012 to 2014 (Table 3) also of moderate spatial resolution Landsat TM (2009 & 2010). Google imageries were also used to measure the accuracy of MODIS snow data. Later both ground sampling and satellite data were used to evaluate the accuracy of snow area.

Table 2. List of Meteorological stations used.

Name of Station	Range of Data	Geographical Location and Elevation		
		Latitude (DD)	Longitude (DD)	Elevation (m)
Khunjerab	1995-2010	36.8500	75.4000	4730
Ziarat	1995-2010	36.8333	74.4333	3669
Naltar	1995-2010	36.2167	74.2667	2810
Shandoor	1995-2010	34.08611	72.525	3719
Deosai	1995-2010	34.95	74.38333	4356

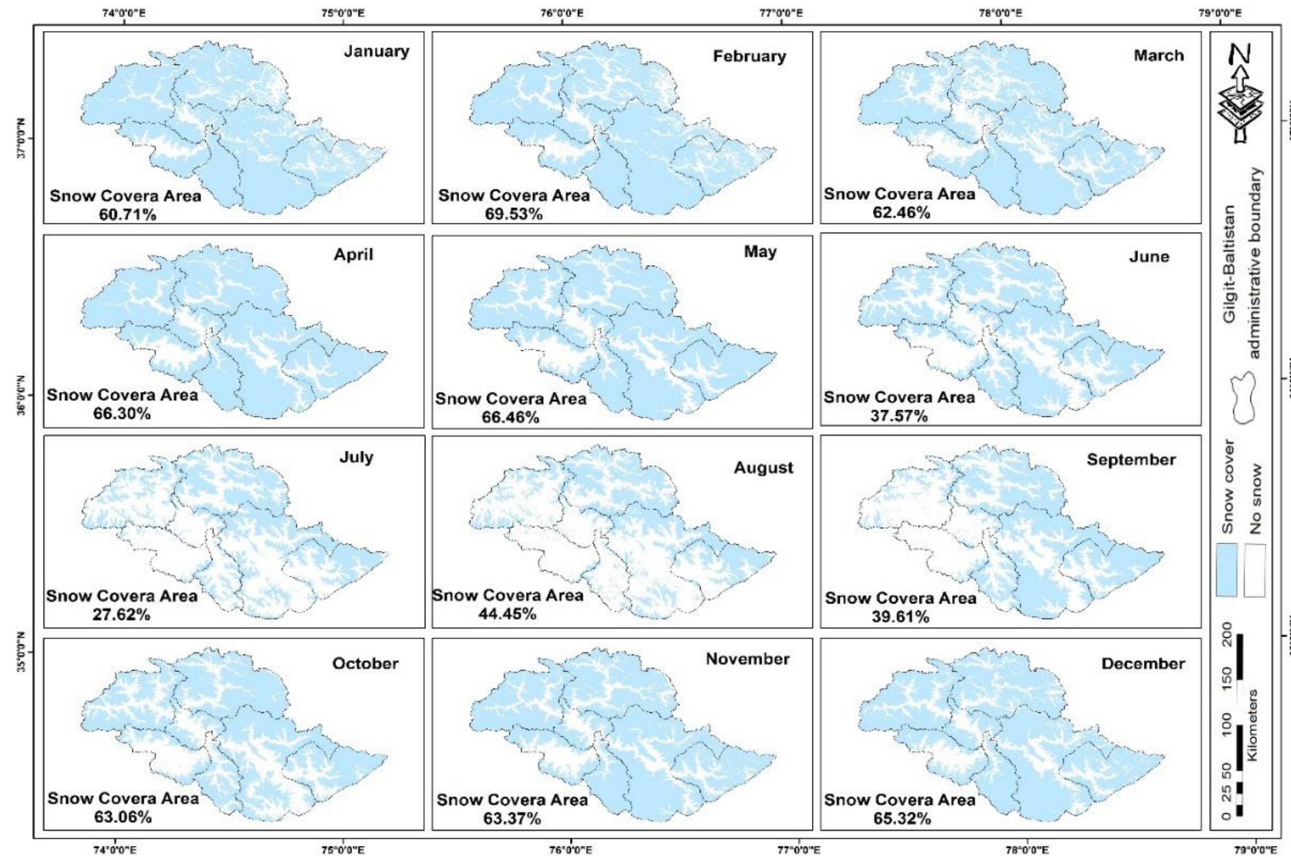

Fig. 3. Monthly average snow-covered of the study area for the period of (2000-2014)

3.3. Cloud removal technique and validation

To minimize the impact of cloud from the authenticated MODIS data, the study computed rigorous non-spectral cloud removal method, partially followed by Wang, Xie, and Liang (2008) and (López-Burgo et al., 2013). The methods used in the above studies found efficient for removal of clouds impact from MODIS snow products and shows good relation with ground snow data. However, these studies propose many cloud removal steps, where each successive step eliminates extra information with clouds, which is noticed that high chance of data damage (Gafurov & Bárdossy, 2009). Here selected some of them with healthy cloud elimination stages, and here discussed their functionality and technical accuracy briefly. In the primary step of cloud removal technique, merged both Terra and Aqua (MODIS) images of the same days to remove short-persevering clouds. The Study mainly focused on MODIS Terra snow data and replace the cloud pixels of the Terra with the corresponding cloud-free Aqua pixel. The resultant of the procedure, we found a single image for the concert day. The technique is more suitable and highly accurate, due to both available observations, datasets are only few hours apart at Equator, such as 3 to 4 hours (Gafurov & Bárdossy, 2009).

Table 3. Ground Sampling points of Snow cover in Gilgit-Baltistan.

S.No	Name	X	Y	S.No	Name	X	Y
1	Astore	74.852884	35.359592	**46**	Thalley	76.156929	35.320764
2	Eidgah	74.856687	35.347248	**47**	Dahir	76.142239	35.338720
3	Eidgah1	74.852910	35.330673	**48**	Chandu	76.167041	35.299326
4	Eidgah2	74.853983	35.321685	**49**	Hushey bridge	76.361497	35.436702
5	Bulan Pine1	74.854506	35.307795	**50**	Hushey	76.359659	35.448278
6	Bulan Pine	74.849147	35.288332	**51**	Hushey 1	76.358646	35.455498
7	Gorikot	74.839424	35.277001	**52**	Kande	76.368027	35.364842
8	Rama	74.826036	35.364042	**53**	Hushey 2	76.354776	35.463621
9	Rama Lake	74.811173	35.359808	**54**	Passu	74.892982	36.465139
10	Viewpoint shigar	75.748219	35.382155	**55**	Hussaini	74.869492	36.423928
11	Hasupikere	75.735195	35.432256	**56**	Borit	74.861884	36.435733
12	Skono	75.709857	35.463750	**57**	Gulkhin	74.865496	36.402593
13	Wazirpur	75.598158	35.517261	**58**	Khudabad	74.798265	36.579886
14	Yonskit	75.548361	35.569564	**59**	Nazimabad	74.865474	36.613369
15	Bien	75.397318	35.752941	**60**	Gircha	74.863030	36.596436
16	Doko	75.399843	35.778440	**61**	Khybar	74.881162	36.494527
17	Zil	75.404954	35.800974	**62**	Ghurbon2	75.039913	36.166197
18	Sesko	75.415501	35.815622	**63**	Ghurbon1	75.035416	36.168650
19	Gupis	73.450520	36.228118	**64**	Ghurbon3	75.045649	36.165460
20	Gupis1	73.440095	36.230006	**65**	Ghurbon	75.031381	36.168982
21	Bridge	73.419227	36.236581	**66**	Hisper	75.002091	36.168767
22	Khalti	73.400004	36.233538	**67**	Hisper	74.998429	36.172764
23	Khalti Lake	73.385086	36.241348	**68**	Hisper	74.989744	36.176919
24	Khalti Lake1	73.375485	36.240797	**69**	Hisper	74.984070	36.178142
25	Khalti Lake2	73.359283	36.243649	**70**	Hisper	74.976957	36.180422
26	Damalgan	73.408558	36.253783	**71**	Hoper	74.746771	36.250042
27	Sandi	73.398817	36.296116	**72**	Shakoshal1	74.737292	36.241391
28	chalt Chaprot	74.256144	36.267889	**73**	Shakoshal	74.729904	36.239956
29	Chaparot	74.264694	36.251960	**74**	Hakashal	74.748431	36.237232
30	Bar	74.284491	36.329616	**75**	Hakashal	74.757323	36.239455
31	Bar Khas	74.294393	36.380540	**76**	Brushal	74.745389	36.225713
32	Bar Khas 1	74.297184	36.440084	**77**	Brushal	74.757625	36.229384
33	Bar Khas2	74.287627	36.449566	**78**	Ghoshoshal	74.754400	36.218244
34	Chalt	74.304477	36.238400	**79**	Ghoshoshal1	74.762751	36.222485
35	Chalt 2	74.321489	36.248510	**80**	Forest hut	74.170074	36.156210
36	Chalt 3	74.348717	36.253976	**81**	Wetland Complex	74.099459	36.233311
37	Ghakuch Payeen	73.768467	36.156780	**82**	Chomobari	74.103386	36.228557
38	Ghakuch Payeen1	73.737218	36.171539	**83**	Oposit site Chomobari	74.112102	36.227093
39	Imit	73.898314	36.503612	**84**	Near Chomobari	74.113896	36.216724
40	Imit Rest House	73.958105	36.512765	**85**	Air Force	74.167071	36.162413
41	Ishkoman	73.854034	36.513747	**86**	Naltar Payeen1	74.186160	36.165312
42	Ishkoman Payeen	73.837107	36.522243	**87**	Naltar Payeen	74.189116	36.162219
43	Ghakuch Bazar	73.729827	36.202750	**88**	Chumarsoo	74.134377	36.206002
44	Ghakuch College	73.724989	36.228985	**89**	Phandar	72.928688	36.167982
45	Ishkoman Bridge	73.864241	36.495225	**90**	Phandar	72.908739	36.155225

As for the temporary filling, in this study replaced the same day pixel (cloud) with immediate previous matching day cloud-free image pixel. In the temporal analysis, if the next and previous both day matched cloud-free pixels detect the same period, the existing day corresponding cloudy pixel is replacing by that tile/class. Here, suppose that the snow area regularly continues more than eight days. Thus, the existing-day pixel (cloud) can be replaced with the same previous day pixel (snow). If the previous eight days' snow acquired from the Aqua snow images as a result of the procedure in step one, then it is a few hours difference from current day cloud pixel.

During the period of snow observation taken by satellite, there are three possibilities such as snow accumulation, ablation, or nor accumulation or ablation. Here is such a limited probability of ablation, due to the day is cloudy, hindering in the way of solar radiation by clouds (Gafurov & Bárdossy, 2009). While snow accumulation or no change are still possibilities in the data as a hypothesis. However, the Terra and Aqua data (snow) is in the right arrangement; these datasets have little variances, mostly throughout the intermediate period (Wang et al., 2009). These changes are identified as to the transformation of a pixel from terrestrial feature to snow in case of snowfall and not reached to ground in terms of ablation during the observation taken a period of Terra and Aqua data (Parajka & Blöschl, 2008). Distribution of snow on the ground also effects by wind direction during the acquisition period of the data. Such type of effects and variation also recorded daily consider in this part of the analysis, because we assume single observation per day for analysis of data. Sometimes this information even loss under exist clear condition of sky. As for spatial replacement/filling, here replaced a specific pixel of the cloud with the transparent pixel from cloud between neighbouring pixels. However, such type of pixel replacement is not accurate, but it increases the probability of image accuracy as high. The main problem is coming in the snow separation in sparse, which provides wrong information. Here we measured the snow distribution in the spatial extent of 7 × 7 m transect, to quickly identify the cloud pixel from data with the available wind of neighbouring pixels. This window size as ideal for the spatial gap-filling to minimize the effect of cloud pixel in MODIS snow data, which is also described by (Gurung et al., 2011). In this research first, merge MODIS Terra and Aqua images, later applied temporal and spatial filling techniques with neighbouring pixels, and at the end, temporal data analysis was done for minimizing the remaining cloud impact from data. Image preprocessing data of MODIS 8-days snow for further snow area measurement and analysis. For the validation of the MODIS snow data, the original form of data was used with relative validation technique. For this purpose, the data of 2004 were taken into account because it was first wet year after a long dry period (drought; 1998/99-2002/03) over the Upper Indus Basin region (Baig & Rasul, 2009). Ten pairs of Terra and Aqua snow images windows were selected from the same day, which has considerable cloud cover differences and converted into cloud-free products after we have applied cloud removal method. The same day Terra and Aqua images are two separate techniques of data acquired with the parallel process at a different time interval of the day (Parajka & Blöschl, 2008). First, the method of masking method was applied on Terra snow data, and the resultant product was compared with the same day Aqua snow data. The remaining portion of the Aqua snow data shows cloud-free in the corresponding same-day Terra snow images. All the steps of the cloud removal method were applied on whole data for produced cloud free product for further analysis. The resultant snow and cloud cover approximations are compared to the measurements from the same day Terra snow image. The MAD; mean absolute difference was calculated by using equation (2). Here we assume cloud removal method performance is suitable if it minimizes cloud cover upto less than 10% for the study area or AOI; area of interest.

$$MAD = \frac{\sum |Snow_{MYD/MOD} - Snow_{Landsat}}{n} \quad 2$$

where SnowMYD/MOD are cloud-free images of MODIS snow data extracted from Terra and Aqua satellite, and Snowlandsat is snow area calculated from Landsat TM images, as well as n, is the total number of the days.

3.4. *Pearson's correlation coefficient analysis*

A non-parametric test "Pearson's correlation coefficient" algorithm was applied for correlation analysis of monthly, seasonal and annual snow-cover with temperature data. Non-parametric statistical trend test was implemented based on the available dataset. The trend magnitude was calculated using Guesses linear regression algorithm with a 95% confidence level. The in-situ climatic parameters (mean temperature) were used for computed correlation between the snow-cover area (monthly %) and different elevation zones. Correlations were further analysed between snow-cover, net radiation and wind speed, for the study area and the period.

4. Results and discussion

The NDSI was computed, and charts were produced for the study period (Fig. 3). The correlation coefficient was calculated between SCA and the mean monthly temperature. Correlation of snow and climatic parameter represented weakest and strongest relationship regions in the study area for different elevation zones.

4.1. *Validation and accuracy assessment of MODIS snow products*

A part of field data collection (Global Positing System; GPS data) during the ground-truthing exercise (collection of GPS point from different selected sites in Gilgit-Baltistan; Table 3) was carried out for accuracy assessment also of satellite images. About 90 ground control points; GCP were taken to compile accuracy of MODIS snow products. The study focused on snow-cover analysis in GB, and it was not possible with GIS and remote sensing technique due to harsh climatic conditions and inaccessible areas of high-altitude perennial snow/ice, and glacier regions. Therefore, only we assumed and collected sampling points from valley bottoms for accuracy assessment of snow cover area. The overall accuracy of the MODIS snow data is 93% against collected GCPs. A similar type of results is also found for the validation period of MODIS snow data against Landsat TM and Google earth images. Overall validation results of MODIS snow data showed good agreement with the Landsat images. The high accuracy of MODIS data for snow-cover analysis are also verified by (Forsythe et al., 2012; Immerzeel et al., 2009; Samreen et al., 2014; Tahir et al., 2011) for the UIB region and Tang et al. (2013), and Hasson et al. (2014) for the Tibetan Plateau region and Western Indus river system respectively.

4.2. *Cloud removal technique and validation*

The cloud removal technique fills up around 76% and 79% of the cloud data gaps in the MODIS Terra and Aqua products, respectively, with an accuracy of 93% against the observations. Similarly, overall efficiency improves by the procedure from the MODIS Terra (88%) and Aqua (86%) products to 89% products. About 16% of gaps filled by the MODIS Terra and Aqua combining steps with an accuracy of around 89 % against the observations (Table 5). The snow miss and false alarm rates for this step are nearby 4% and 7% respectively. The remaining steps (temporary filling, spatial filling and temporal analysis) have around filled up 65, 8 and 14% respectively, of the total filled data gaps with an accuracy of 93% against the observations. From Table 2 explain that considerably the clouds from the Aqua images have been reduced, and the snow estimates have improved accordingly, which are now comparable to the MODIS Terra estimates. About 0.54% MAD between the MODIS Terra and Aqua snow estimates. It may partly be attributed to same-day Terra and Aqua images spatial cloud/snow cover differences, as shown in Table 2. It is also partially because the cloud has been not eliminated from the Aqua images. After all, the first step (in combining both same-day images) has been skipped during this validation process. During the whole validation period of the years 2005, the applied cloud removal technique has reduced the effect of cloud cover from MODIS Terra 37% and MODIS Aqua 43% to 7%. Similarly refining snow-cover estimates from 7% MODIS Terra and 5 % MODIS Aqua to 14% for the whole study area. For all the individual steps (image combining, temporal filling, the spatial filling, and temporal analysis) have reduced the impact of average cloud cover around 19, 9, 8, and 7%, as well as improve the result and quality of the snow-cover images around 8, 12, 13, and 14% respectively for the UIB region (Fig. 4).

4.3. Snow cover estimates and distribution of precipitation

Figure 6 describes the total SCA for every eight days at six different elevation zones, and chart values represent the average SC for the study period (2000-2014). From the results, it is not always tediously increased with change of elevation in the region. These results are used to draw the snow-melting curve. Usually, these are used for snow-melt runoff modelling. From the figure, a clear partitioning of elevation zones from low (below 2000m) to higher (6000 m and above) is visible. In the lower elevation zone, snow cover is <40% throughout the year except for winter months (3000m-400 m elevation zone), while it is >60% in upper elevation zone throughout the year. During the winter season, particularly in February and March snow cover area is higher at elevation Zone III as compared to Zones IV and V. For the remaining months of the year snow cover has smoothly increased with increasing elevation in the elevation zones. Figure 5 indicated large snow extent for summer as compared to winter in high elevation zones (6000m) probably due to cloud cover during the winter season.

Table 4. Overall accuracy and Kappa (κ) statistics for the classifications for the period 2000 to 2014.

	2000		**2005**		**2010**		**2014**	
Classification	**Producer**	**User**	**Producer**	**User**	**Producer**	**User**	**Producer**	**User**
Snow cover	93.3	93.3	93.3	96.6	93.3	90.3	93.3	87.5
No Snow	96.7	85.3	96.7	59.2	93.3	77.8	93.3	65.1
Overall	95.00		95.00		93.3		**93.3**	
Kappa	92		76.6		87.8		**78.9**	

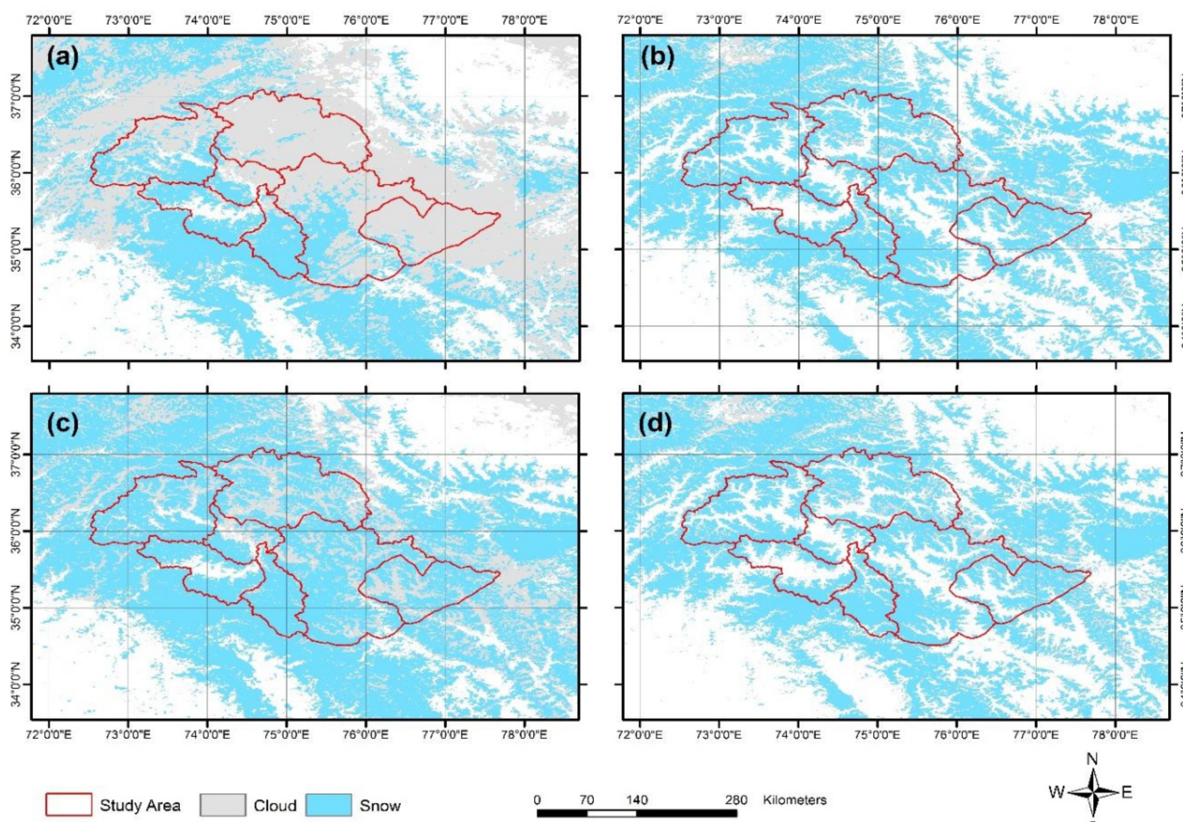

Fig. 4. Cloud and snow-cover of Original MODIS Terra and Aqua images and after implementation of the cloud removal steps for the year 2005, a) MODIS Terra image, (b) MODIS Aqua image, (c) After combining Terra and Aqua (d) After temporal, spatial filling and temporal analysis.

Figure 7 (box-plots) shows monthly snow cover per cent variation in different elevation zones for the study period (2000-2014) revealing a large inter-annual variability in the snow cover extent, particularly during winter. Zone III (3000-4000m) had maximum (up to 60% in February) snow variation in winter months, which shows the highly inconsistent repetition of substantial snow-fall intervals in January and February, sometimes repeated in the same pattern after several years for December and March at the same elevation. This is also correct for elevation zones IV and V (4000-5000m and 5000-6000 m) that have relatively large inconsistency in winter snowfall intervals. It is often challenging to measure snow cover depth in this region as the wind speed and direction greatly influence snow distribution and hence snow cover. In the winter season, in zone VI (>6000 m) showed considerable variation in snow cover, which is the reason snow-cover area was as large as 40% in February and March at lower elevation zones. However, another factor for variation in these elevation zones was relatively large per cent of cloud-cover in the winter season, which influenced snow pixels' detection in imageries. For the elevation zone VI (>6000m) a comparatively low inconsistency was observed during the three seasons except for summer, in snow cover variability between zone V and zoneVI.

4.3. Snow cover trends analysis

Modis 8-day snow cover product was analysed and evaluated with NDSI (Equation-I) value ≥ 0.4 was consider as snow for the study period. Pearson Coefficient correlation trend was computed for the periodical such as annual, monthly and seasonal snow cover change analysis for the period of 2000-2014. Trend results and their slope with a confidence level of

Pearson Coefficient correlation trend was computed for the periodical (monthly and annual) and seasonal snow-cover change analysis for the study period (2000-2014) with elevation zones. The results of trends and their slope with a confidence level of 95% are represented in Table 5. Although 15 years period is considered not enough to calculate the excellent trend results from such an analysis, still there was some good, and reasonable high correlation trends were founded in the region. From the results, there is a decreasing snow cover trend in December and January, and also indicated an increasing trend for February and March of each year.

Table 5. Results of the MODIS Terra and Aqua snow products validation against the Landsat images.

Months	MODIS Terra Snow Cover Area (Km^2)	Landsat Images Snow Cover Area (Km^2)	Relative diff (%)	MODIS Aqua Snow Cover Area (Km^2)	Landsat Images Snow Cover Area (Km^2)	Relative diff (%)
Jan	0	0	0			
Feb	0	0	0			
Mar	4504.95	4236.40	6.34	10878	10238	6.26
Apr	7128.71	7740.59	-7.90	21407	19654	8.92
May	8118.81	7531.38	7.80			
Jun	12623.76	13750.00	-8.19			
Jul	13168.32	12866.11	2.35			
Aug	15099.01	15428.87	-2.14			
Sep	19356.44	19351.46	0.03	249	335	-25.59
Oct	20396.04	19194.56	6.26	924	594	55.52
Nov	21188.12	19769.87	7.17	798	1056	-24.46

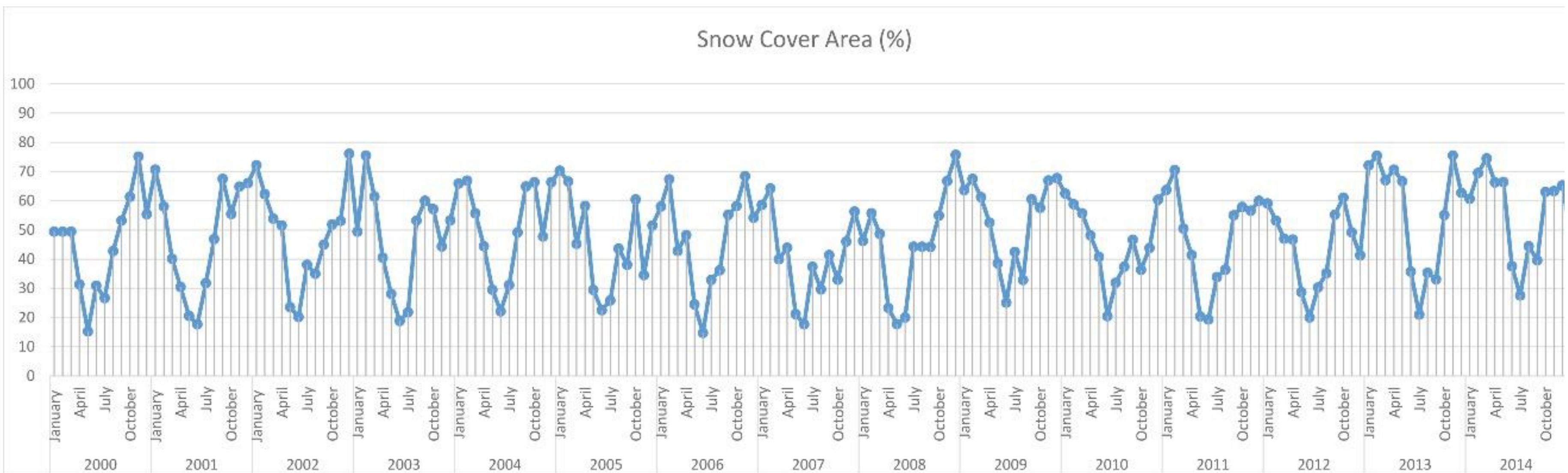

Fig. 5. Monthly snow cover variation in the study area (x-axis represents months and years, and the y-axis represents snow cover area in % age)

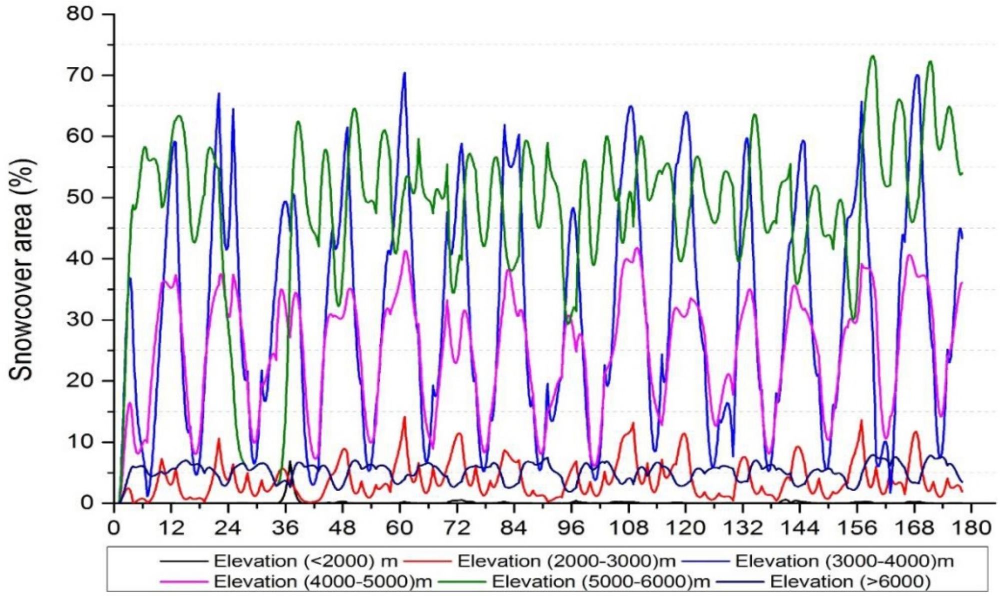

Fig. 6. Monthly snow cover variation in the study area with different elevation.

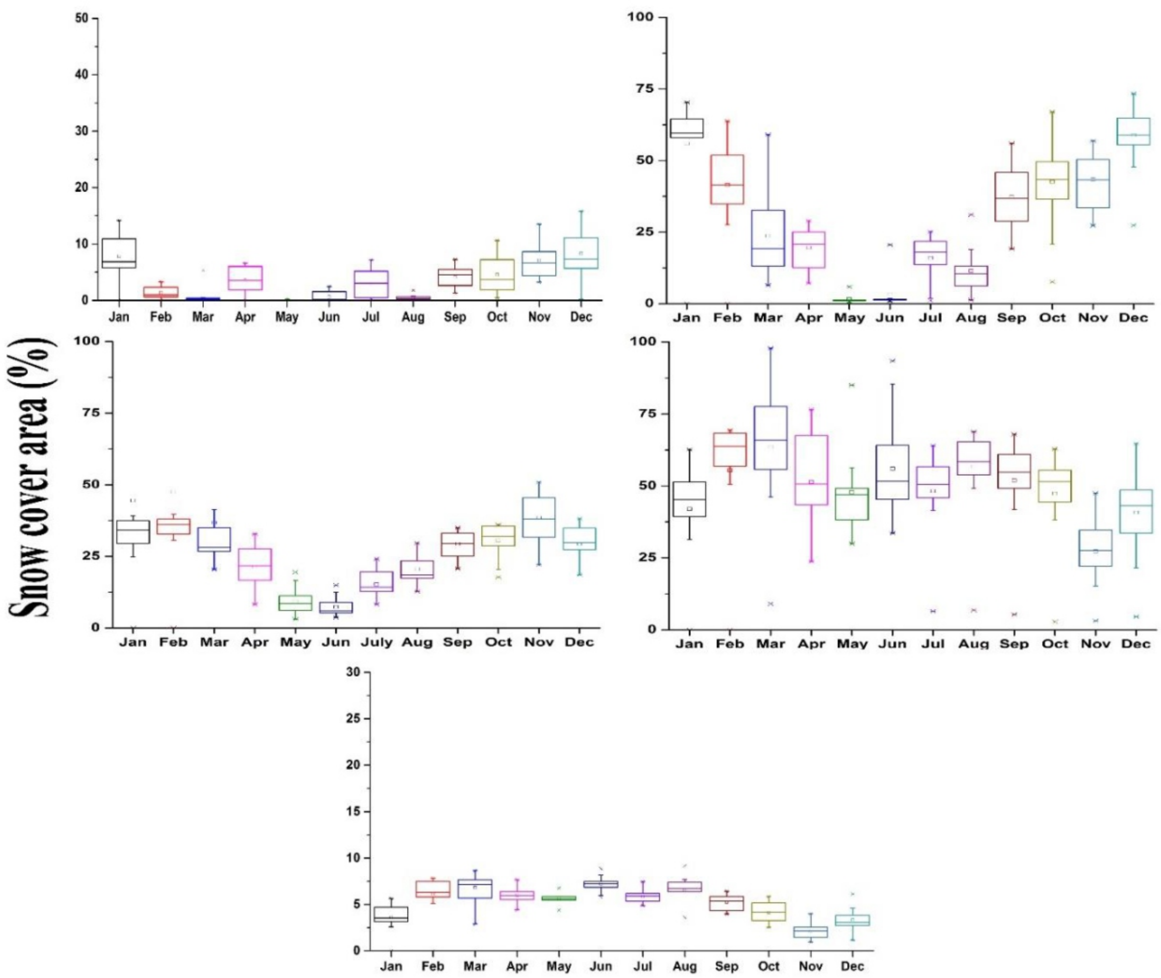

Fig. 7. Box-plot represented the monthly snow cover variations in (%), in the study area for 15-years (2000 to 2014).

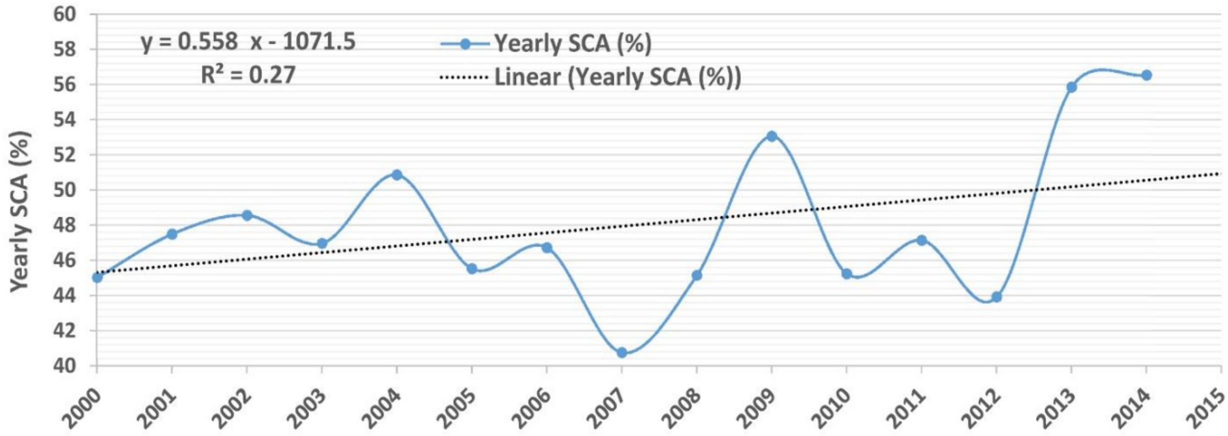

Fig. 8. Yearly (2000-2014) snow cover trend in the study area.

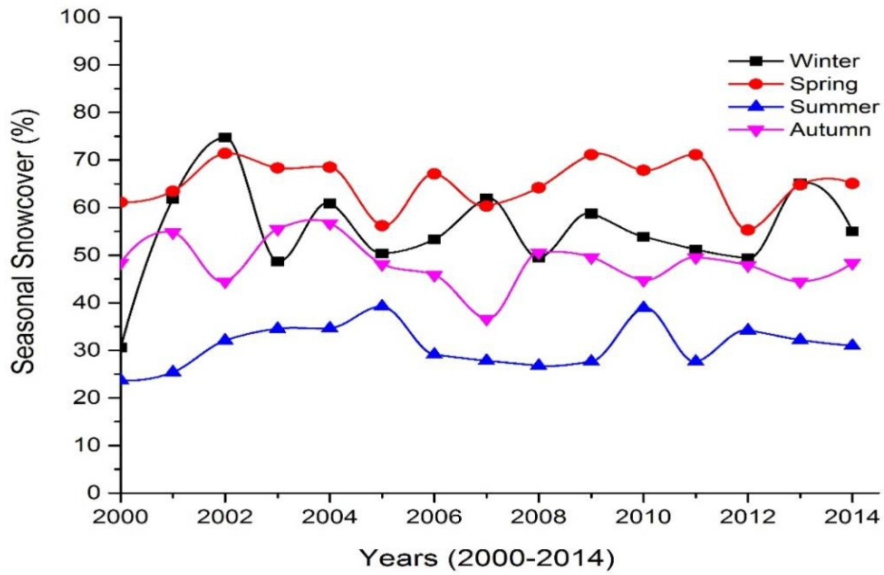

Fig. 9. Seasonal snow cover variation (2000-2014); x-axis represented years, and y-axis represented snow cover in percentage (%).

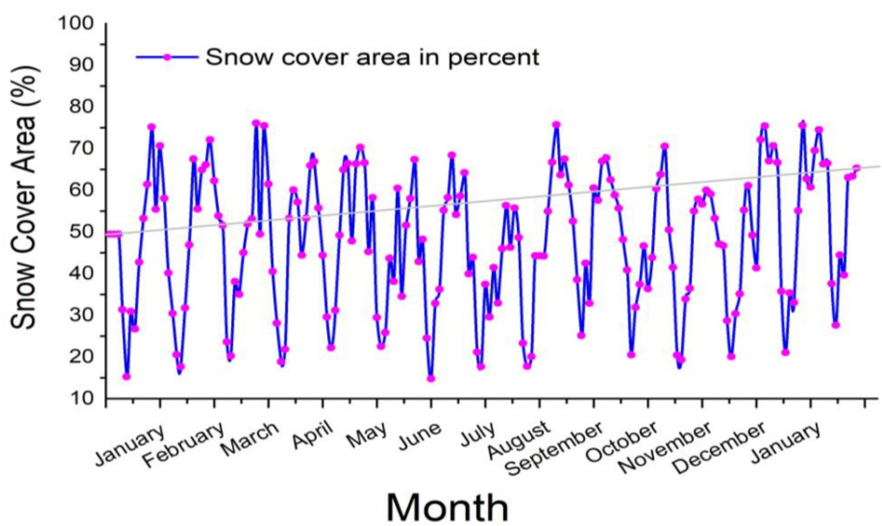

Fig.10. Monthly snow cover trend in the study region for years (2000-2014); a-axis represents months, and the y-axis represents snow cover area in percentage (%).

For seasonal level correlation analysis, the results showed negative winter trend for the elevation zones above 3000m to 6000m, and also similar pattern was founded for elevation zone III and IV in spring. On the other hand, increasing trends were observed for all zones above 4000m for the autumn season. If such trends were observed for snow cover, resultant noticeable variations would have occurred in spring and autumn discharge, and stream and river flow, with a positive impact on flow patterns downstream. Elevation zones in the range of 5000m ASL are more sensitive to climate change, a majority of the HKH glaciers, snow and ice masses are present in this elevation zone, and also a significant portion of the land above 5000m ASL remains covered with perennial and non-perennial snow throughout the year. Therefore, even a minor change in the freezing / melting thresholds in this elevation regime could have a significant impact on snow melting in the region. The area above 7000m ASL is also crucial for snow accumulation trends as snow-cover increasing trends were observed at high elevation zones mainly during winter seasons in the UIB area (Immerzeel et al., 2009). Some new results about snow cover change analysis in the region (Gilgit-Baltistan of UIB) were represented in the below figures. Snow cover changes in between years 2000 and 2014, and also yearly, seasonally and monthly snow cover trend are shown in Figure 8, 9 and ten, respectively for the study period.

4.5. Pearson's correlation coefficient between SCA (%) and Temperature

Monthly correlations between snow and temperature represented in figure 11 and 12, were computed form the high altitude ground stations (in-situ temperature) installed at Deosai, Khunjerab, Naltar, and Shandoor. For maximum snow cover area (%) showed negative correlations with the mean temperature for same and previous no-snowing months, for instance, November and January below 6000m ASL (Zone I - V) in the study area. Figure 11 and 12 represented the selected months with their high correlations between snow-cover and temperature according to their importance. These results also explained the MODIS snow product distribution trend with the consistency of the snow-product for the region. From table 5, a high negative correlation between snow and temperature shows the decreasing trend of snow in the area. For example, a highly negative correlation was founded between snow and temperature means, showing a decreasing snow cover trend in January for all elevation zones above 2000m ASL., which means higher temperature was observed during the period of last December and January. Weather data (temperature) from ground stations and snow cover (%) for the same period showed increasing trends in December (p=+0.88) and January (p=+0.52) respectively. Similarly, a positive correlation between snow cover in November as a result of decreasing temperature trends were observed in October and November (p= −0.27) for the study area.

4.6. Regression analysis

Dependent snow cover area and independent weather data (mean temperature) were analyzed using multi-linear regression analysis algorithm as below:

$$\boldsymbol{Y = XI + X2 + X3 + S} \qquad \mathbf{2}$$

Where Y= snow cover, X1, X2 are respective maximum and minimum temperatures. X3 is a constant snow variable.

The results of regression analysis (R2 = 0.661) indicated that, about 66% of the snow cover dependents on available climatic variables. Regression analyses were computed (equation 2) for the prediction of variation in long term snow cover dynamics in the region with different climatic parameters. From the results, it was revealed that the snow/ice cover remains constant with a slight change in ice volume, but will be in future it will be decreasing. Similar results also described by for the Hunza river basin as well as the elevation of snow equilibrium line shifted towards 5500m elevation to 5800 m ASL., which presently exists according to results of , which is placed around 5200m ASL.

Table 5. Pearson Coefficient correlation trend for the study area at different elevation zones.

Indicators	Elevations (m)											
	<2000		2000-3000		3000-4000		4000-5000		5000-6000		>6000	
	[redacted]	Slope	[redacted]	slope	[redacted]	slope	[redacted]	slope	[redacted]	slope	[redacted]	slope
Jan	-0.25	−3.03±5.98	-0.13	−2.71±3.17	-0.02	**−2.61±2.45**	-0.14	n.a.	0.11	n.a.	0.09	−3.03±5.98
Feb	0.34	n.a.	0.39	--	**0.61**	+0.84±3.41	-0.01	n.a.	**0.60**	**+0.44±0.86**	**0.73**	**+0.18±0.19**
Mar	0.03	−0.78±5.45	-0.44	−0.34±2.70	-0.33	+0.11±3.40	-0.05	+0.52±0.89	0.06	n.a.	0.23	−0.78±5.45
Apr	-0.07	--	-0.16	−0.24±1.55	-0.17	−0.37±1.88	-0.07	−0.12±0.57	-0.04	n.a.	-0.03	--
May	0.03	n.a.	0.37	−0.43±0.92	0.01	−0.87±2.08	-0.29	−0.40±0.91	-0.49	+0.19±0.65	-0.45	n.a.
Jun	-0.40	n.a.	0.43	−0.12±0.14	-0.06	−0.14±0.78	-0.43	n.a.	-0.08	+0.44±0.86	0.18	n.a.
Jul	-0.04	n.a.	-0.44	n.a.	-0.22	n.a.	0.01	n.a.	0.15	n.a.	**-0.52**	**−0.12±0.14**
Aug	0.21	n.a.	0.03	n.a.	-0.20	n.a.	-0.42	n.a.	-0.23	n.a.	0.06	n.a.
Sep	**0.79**	**+0.51±1.64**	0.34	+0.18±0.19	0.16	--	0.04	−0.28±1.37	0.27	+0.09±0.61	-0.45	n.a.
Oct	0.01	n.a.	0.14	+1.06±1.65	-0.06	+1.37±2.90	0.11	--	0.05	−0.12±0.59	0.33	**+0.51±1.64**
Nov	0.34	−0.20±0.96	0.23	+0.35±1.62	0.02	+0.87±3.09	0.37	+0.12±0.84	-0.28	+0.10±0.76	-0.18	−0.20±0.96
Dec	-0.10	--	0.15	−0.25±1.65	0.25	--	**0.51**	**+0.52±0.89**	-0.05	n.a.	0.05	--

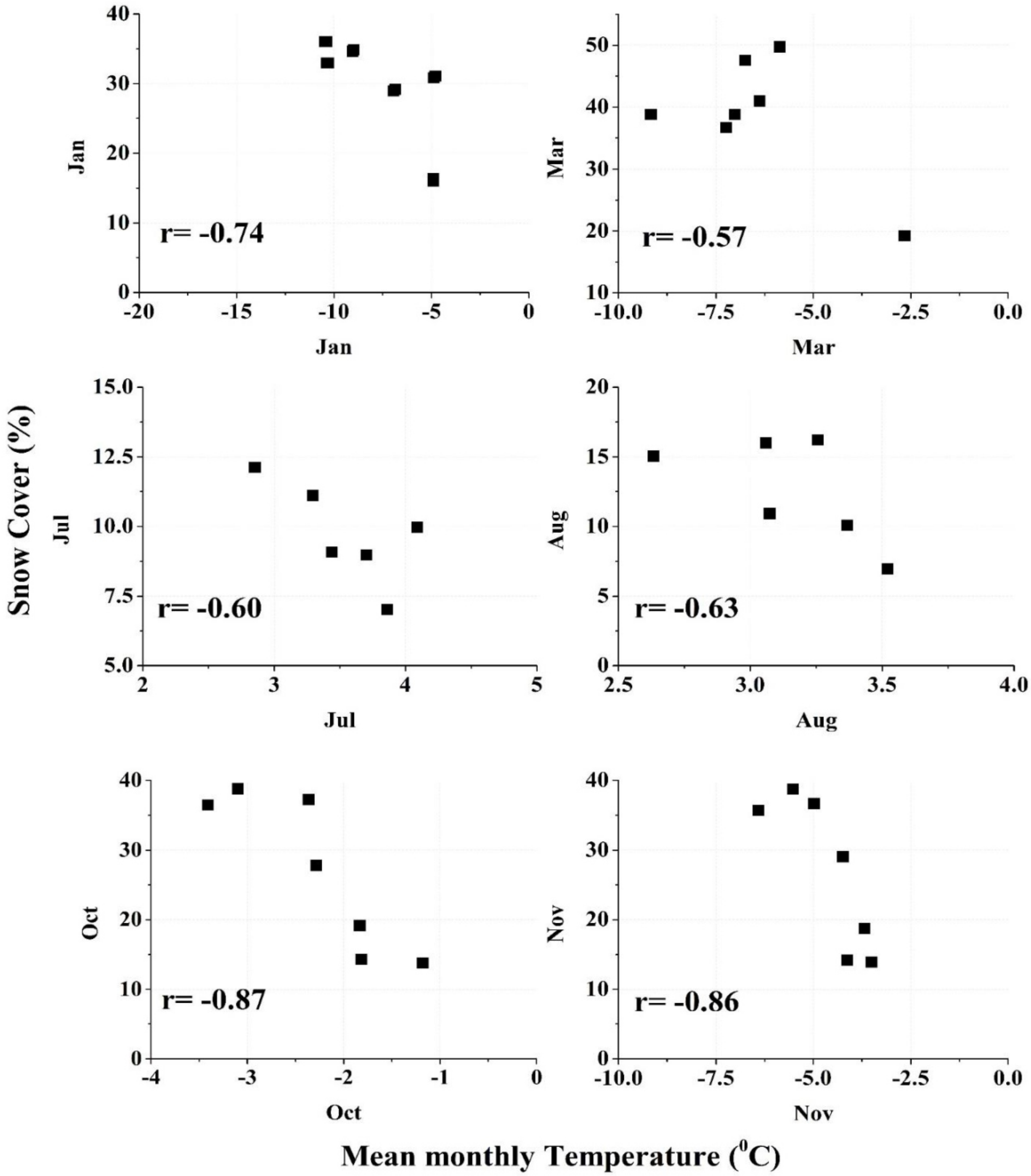

Fig. 11. Correlations between monthly snow cover (%) at 5000-6000 m elevation zone and monthly temperature at the Khunjerab station at elevation 5182 m. The r values in bold are significant at 5% confidence level (a-axis of the diagram represents monthly mean temperature and y-axis represents snow cover area in percentage (%) for specific correlation months)

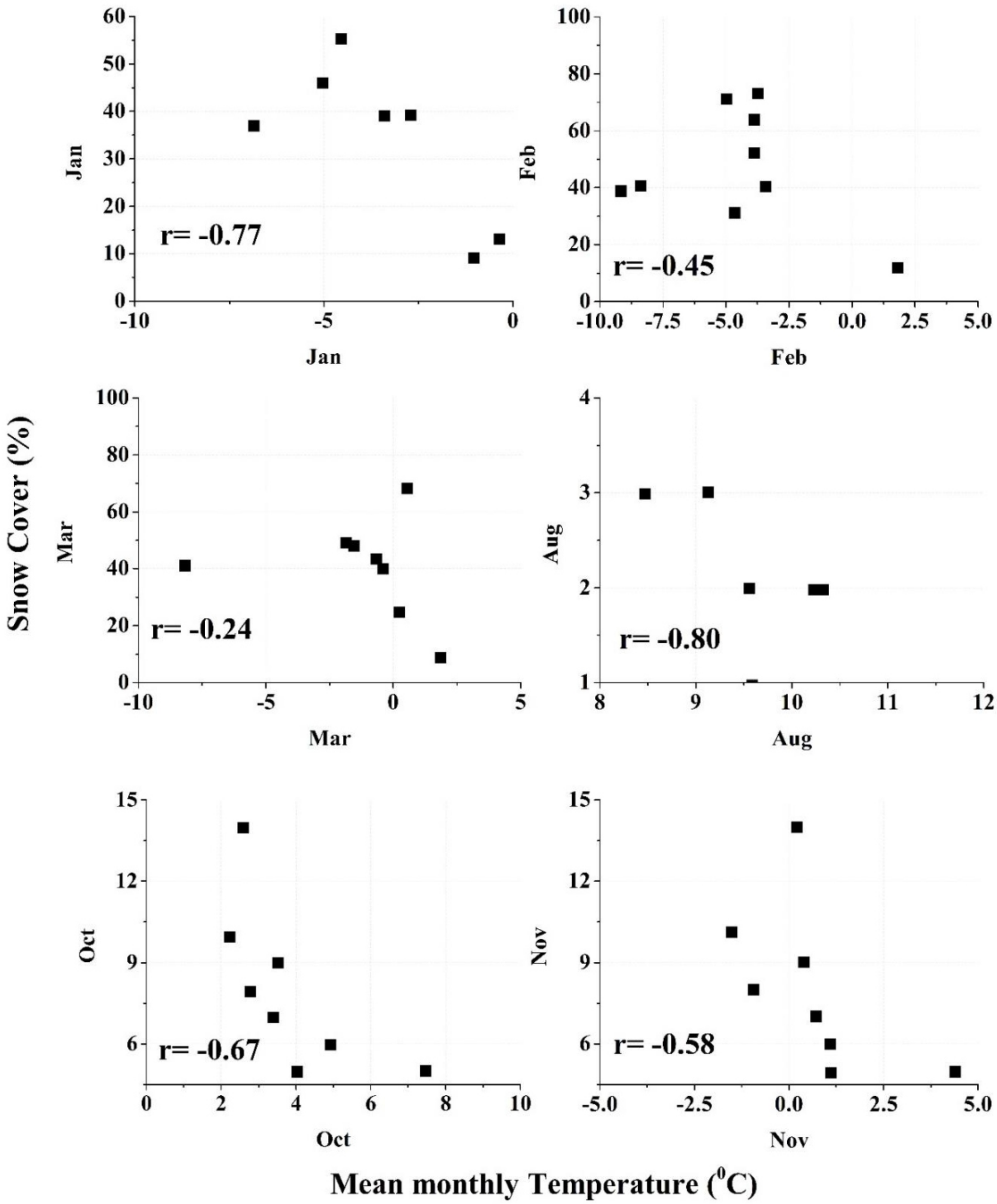

Fig. 12. Correlations between monthly snow cover (%) at 3000-4000 m elevation zone and monthly temperature at the Deosai station at elevation 4356 m. The r values in bold are significant at 5% confidence level (a-axis of the diagram represents monthly mean temperature and y-axis represents snow cover area in percentage (%) for specific correlation months).

5. Conclusions

The snow cover change analysis trends for the last 15 years (2000-2014) shows some impressive results. Results are indicated an increasing trend of snow cover in March instead of January (Fig. 11) which may directly affect on river flow in the region and their availability of water resources, mainly in spring season when water needs for an irrigation system for its peak. Seasonal trends were indicating a negative trend for winter, particularly in elevation Zone III, IV and V, while increasing trends were found in all zones above 4000m ASL for autumn season (September-November). Although it is challenging to determine variability in hydrological regimes (water resources) of the region, some of the results from the predicted trends of snow cover indicate strong correlations between prevailing weather conditions and snow cover area. Mainly decreasing trends in snow cover was founded for January, and an increasing trend for November probably due to slightly increase in mean temperature in the previous December and January months. A decreasing trend in temperature was observed for past November in the study area. Negative correlations observed between snow cover area and temperature verified the validity of MODIS data. Whether these patterns will continue as other years of data gathering to be available stays to be seen. However, these outcomes indicate the importance of satellite-based snow products, and need of monitoring the change of selected ice sheets and glaciers, as well as it is more valuable and essential to monitor regional extent of the snow/ice or glaciers spread for more reasonable valuation to fate of the available crucial freshwater resources presented in HKH region. Due to reliability and increased use of MODIS snow product for snow cover analysis serve as a valuable asset for evaluating climate change impact of highly inaccessible HKH mountain region. It must be noted here that, the snow cover not only impact the snow-melt but water equivalent and snow-depth, also impact on cryosphere melting, and indirectly effect on water resources and Indus river system flows down-streams later. Therefore, these factors must be considered in all future studies, for reliable results from the Karakoram ice mass assessments, to understand better its impact on downstream flows and water contribution into Indus River system for sustainable water management in UIB of Pakistan.

Acknowledgment

This study is funded by Xinjiang Institute of Ecology and Geography, Chinese Academy of Science, Urumqi 830011 and University of the Chinese Academy of Sciences (UCAS), Beijing. Authors acknowledge the Pakistan Meteorological Department (PMD) and the Water and Power Development Authority (WAPDA)-GoP, for providing climate datasets for the study area. We also thank the unknown reviewers for their valuable comments and suggestions for improving the draft manuscript.

Author's Contribution

Garee Khan, developed main concept of research and involved in write manuscript. Chen Xi, supervised the study whole study and assisted in establishing graphs and maps. Babar Khan, help in modification and editing of writing. Javed Akhter Qureshi, collected field data. Hawas Khan did provision of relevant literature, and review. Muhamad Alam did review before submission and proof read of the manuscript.

References

Ashraf, A., Ahmad, S. S., Aziz, N., Shah, M. T. A., 2012. Preliminary Estimation of Snow Covers Extents of Astore River Basin in Northern Areas, Pakistan. Journal of Geography and Geology, 4(2), 124.

Baig, M. H. A., Rasul, G., 2009. The effect of Eurasian snow cover on the monsoon rainfall of Pakistan. Pakistan J. Meteorol, 5, 1-11.

Barnett, T. P., Adam, J. C., Lettenmaier, D. P., 2005. Potential impacts of a warming climate on water availability in snow-dominated regions. Nature, 438(7066), 303-309.

Bashir, F., Rasul, G., 2010. Estimation of average snow cover over northern Pakistan. Pakistan Journal of Meteorology, 7(13), 63-69.

Bhambri, R., Bolch, T., Kawishwar, P., Dobhal, D., Srivastava, D., Pratap, B., 2013.

Heterogeneity in glacier response in the upper Shyok valley, northeast Karakoram. The Cryosphere, 7(5), 1385-1398.
Bocchiola, D., Diolaiuti, G., 2013. Recent (1980–2009) evidence of climate change in the upper Karakoram, Pakistan. Theoretical and applied climatology, 113(3-4), 611-641.
Bolch, T., Kulkarni, A., Kääb, A., Huggel, C., Paul, F., Cogley, J. G., Scheel, M., 2012. The state and fate of Himalayan glaciers. Science, 336(6079), 310-314.
Dietz, A. J., Wohner, C., Kuenzer, C., 2012. European snow cover characteristics between 2000 and 2011 derived from improved MODIS daily snow cover products. Remote Sensing, 4(8), 2432-2454.
Diodato, N., Bellocchi, G., Tartari, G., 2012. How do Himalayan areas respond to global warming? International Journal of Climatology, 32(7), 975-982.
ESRI, R., 2011. ArcGIS desktop 10. Environmental Systems Research Institute, CA.
Forsythe, N., Fowler, H. J., Kilsby, C. G., Archer, D. R., 2012. Opportunities from remote sensing for supporting water resources management in village/valley scale catchments in the Upper Indus Basin. Water Resources Management, 26(4), 845-871.
Forsythe, N., Kilsby, C. G., Fowler, H. J., Archer, D. R., 2012. Assessment of Runoff Sensitivity in the Upper Indus Basin to Interannual Climate Variability and Potential Change Using MODIS Satellite Data Products. Mountain Research and Development, 32(1), 16-29. doi:10.1659/mrd-journal-d-11-00027.1
Foster, J. L., Hall, D. K., Eylander, J. B., Riggs, G. A., Nghiem, S. V., Tedesco, M., Casey, K. A., 2011. A blended global snow product using visible, passive microwave and scatterometer satellite data. International Journal of Remote Sensing, 32(5), 1371-1395.
Fowler, H., Archer, D., 2006. Conflicting signals of climatic change in the Upper Indus Basin. Journal of Climate, 19(17), 4276-4293.
Gafurov, A., Bárdossy, A., 2009. Cloud removal methodology from MODIS snow cover product. Hydrology and Earth System Sciences, 13(7), 1361-1373.
Gioli, G., Khan, T., Scheffran, J., 2014. Climatic and environmental change in the Karakoram: making sense of community perceptions and adaptation strategies. Regional environmental change, 14(3), 1151-1162.
Gurung, D. R., Kulkarni, A. V., Giriraj, A., Aung, K. S., Shrestha, B., 2011. Monitoring of seasonal snow cover in Bhutan using remote sensing technique. Current Science (Bangalore), 101(10), 1364-1370.
Hall, D. K., Riggs, G. A., Foster, J. L., Kumar, S. V., 2010. Development and evaluation of a cloud-gap-filled MODIS daily snow-cover product. Remote Sensing of Environment, 114(3), 496-503.
Hasson, S., Lucarini, V., Pascale, S., 2013. Hydrological cycle over South and Southeast Asian river basins as simulated by PCMDI/CMIP3 experiments. Earth Syst. Dynam., 4(2), 199-217. doi:10.5194/esd-4-199-2013
Hasson, S., Lucarini, V., Pascale, S., Böhner, J., 2014. Seasonality of the hydrological cycle in major South and Southeast Asian river basins as simulated by PCMDI/CMIP3 experiments. Earth Syst. Dynam., 5(1), 67-87. doi:10.5194/esd-5-67-2014
Hewitt, K., 2007. Tributary glacier surges: an exceptional concentration at Panmah Glacier, Karakoram Himalaya. Journal of Glaciology, 53(181), 181-188.
Hüsler, F., Jonas, T., Riffler, M., Musial, J., Wunderle, S., 2014. A satellite-based snow cover climatology (1985–2011) for the European Alps derived from AVHRR data. The Cryosphere, 8(1), 73-90.
Immerzeel, W., Pellicciotti, F., Bierkens, M., 2013. Rising river flows throughout the twenty-first century in two Himalayan glacierized watersheds. Nature geoscience, 6(9), 742-745.
Immerzeel, W. W., Droogers, P., De Jong, S., Bierkens, M., 2009. Large-scale monitoring of snow cover and runoff simulation in Himalayan river basins using remote sensing. Remote Sensing of Environment, 113(1), 40-49.

Immerzeel, W. W., Van Beek, L. P., Bierkens, M. F., 2010. Climate change will affect the Asian water towers. Science, 328(5984), 1382-1385.

Khan, B., 2013. Rangelands of Gilgit-Baltistan and Azad Jammu & Kashmir, Pakistan – current status, values and challenges. FAO Report, 45.

Klein, A. G., Barnett, A. C., 2003. Validation of daily MODIS snow cover maps of the Upper Rio Grande River Basin for the 2000–2001 snow year. Remote Sensing of Environment, 86(2), 162-176.

Konz, M., Finger, D., Buergi, C., Normand, S., Immerzeel, W., Merz, J., Burlando, P., 2010. Calibration of a distributed hydrological model for simulations of remote glacierized Himalayan catchments using MODIS snow cover data. Global Change: Facing Risks and Threats to Water Resources, 340, 465-473.

López-Burgos, V., Gupta, H. V., Clark, M., 2013. Reducing cloud obscuration of MODIS snow cover area products by combining spatio-temporal techniques with a probability of snow approach. Hydrology and Earth System Sciences, 17(5), 1809-1823.

Lopez, P., Sirguey, P., Arnaud, Y., Pouyaud, B., Chevallier, P., 2008. Snow cover monitoring in the Northern Patagonia Icefield using MODIS satellite images (2000–2006). Global and Planetary Change, 61(3), 103-116.

Maskey, S., Uhlenbrook, S., Ojha, S., 2011. An analysis of snow cover changes in the Himalayan region using MODIS snow products and in-situ temperature data. Climatic Change, 108(1-2), 391-400.

Mayer, C., Lambrecht, A., Belo, M., Smiraglia, C., Diolaiuti, G., 2006. Glaciological characteristics of the ablation zone of Baltoro glacier, Karakoram, Pakistan. Annals of Glaciology, 43(1), 123-131.

Menon, S., Koch, D., Beig, G., Sahu, S., Fasullo, J., Orlikowski, D., 2010. Black carbon aerosols and the third polar ice cap. Atmospheric Chemistry and Physics, 10(10), 4559-4571.

Parajka, J., Blöschl, G., 2008. Spatio-temporal combination of MODIS images–potential for snow cover mapping. Water Resources Research, 44(3).

Parajka, J., Pepe, M., Rampini, A., Rossi, S., Blöschl, G., 2010. A regional snow-line method for estimating snow cover from MODIS during cloud cover. Journal of Hydrology, 381(3), 203-212.

Roy, A., Royer, A., Turcotte, R., 2010. Improvement of springtime streamflow simulations in a boreal environment by incorporating snow-covered area derived from remote sensing data. Journal of hydrology, 390(1), 35-44.

Samreen, A. H., Bilal, M., Pervez, A., Tahir, A. A., 2014. Remote Sensing Data Application to Monitor Snow Cover Variation and Hydrological Regime in a Poorly Gauged River Catchment-Northern Pakistan. International Journal of Geosciences, 5(1), 27.

Tahir, A., Chevallier, P., Arnaud, Y., Ahmad, B., 2011. Snow cover dynamics and hydrological regime of the Hunza River basin, Karakoram Range, Northern Pakistan. Hydrology and Earth System Sciences, 15(7), 2259-2274.

Tait, A. B., Barton, J. S., Hall, D. K., 2001. A prototype MODIS-SSM/I snow-mapping algorithm. International Journal of Remote Sensing, 22(17), 3275-3284.

Tang, B. H., Shrestha, B., Li, Z. L., Liu, G., Ouyang, H., Gurung, D. R., San Aung, K., 2013. Determination of snow cover from MODIS data for the Tibetan Plateau region. International Journal of Applied Earth Observation and Geoinformation, 21, 356-365.

Thirel, G., Notarnicola, C., Kalas, M., Zebisch, M., Schellenberger, T., Tetzlaff, A., de Roo, A., 2012. Assessing the quality of a real-time snow cover area product for hydrological applications. Remote Sensing of Environment, 127, 271-287.

Tong, J., Déry, S., Jackson, P., 2009. Topographic control of snow distribution in an alpine watershed of western Canada inferred from spatially-filtered MODIS snow products. Hydrology and Earth System Sciences, 13(3), 319-326.

Treydte, K. S., Schleser, G. H., Helle, G., Frank, D. C., Winiger, M., Haug, G. H., Esper, J., 2006. The twentieth century was the wettest period in northern Pakistan over the past millennium. Nature, 440(7088), 1179-1182.

Wang, X., Xie, H., 2009. New methods for studying the spatiotemporal variation of snow cover based on combination products of MODIS Terra and Aqua. Journal of Hydrology, 371(1), 192-200.

Wang, X., Xie, H., Liang, T., 2008. Evaluation of MODIS snow cover and cloud mask and its application in Northern Xinjiang, China. Remote Sensing of Environment, 112(4), 1497-1513.

Wang, X., Xie, H., Liang, T., Huang, X., 2009. Comparison and validation of MODIS standard and new combination of Terra and Aqua snow cover products in northern Xinjiang, China. Hydrological Processes, 23(3), 419.

Xie, H., Wang, X., Liang, T., 2009. Development and assessment of combined Terra and Aqua snow cover products in Colorado Plateau, USA and northern Xinjiang, China. Journal of Applied Remote Sensing, 3(1), 033559-033559-033514.